Proceedings of the ASME 2018 37th International Conference on Ocean, Offshore and Arctic Engineering
OMAE2018
June 17-22, 2018, Madrid, Spain

OMAE2018-78571

An Analytical Model of Floating Offshore Wind Turbine Blades Considering Bending-torsion Coupling Effect

Xiaoqi Qu
State Key Laboratory of Hydraulic Engineering Simulation and Safety, Tianjin University
Tianjin, China
Email: quxiaoqi_tju@hotmail.com

Yougang TANG*
State Key Laboratory of Hydraulic Engineering Simulation and Safety, Tianjin University
Tianjin, China
Email: tangyougang_td@163.com

Zhen GAO
Department of Marine Technology
Norwegian University of Science and Technology
Trondheim, 7491, Norway Email:
zhen.gao@ntnu.no

Yan LI
State Key Laboratory of Hydraulic Engineering Simulation and Safety, Tianjin University
Tianjin, China
Email: liyan_0323@tju.edu.cn

Liqin LIU
State Key Laboratory of Hydraulic Engineering Simulation and Safety, Tianjin University
Tianjin, China
Email: liuliqin@tju.edu.cn

ABSTRACT

In this paper, an analytical model is proposed to describe the nonlinear vibration of blades on floating offshore wind turbine (FOWT). The bending-torsion coupling equations are derived based on Hamilton's principle. Comparing with the classical Newtonian method, this approach is more mathematically rigorous and systematic. The flapwise and edgewise deformation, the torsion as well as axial extension of the blades are all included in the model. A set of partial differential equations governing the coupled nonlinear vibration is established, and the results are compared with the multi-body model. Some details about the solution of equations are discussed. The eigen values of a rotating blade is also calculated. The structural model proposed in this paper can be widely used in the future study. For example, it can be coupled with an aerodynamic model to study the aeroelastic properties of the wind turbine blades. The effect of platform motion on blade dynamic response can also be obtained based on this analytical model.

INTRODUCTION

Wind energy development has been paid more and more attention these years because of its contribution of relief the global warming and energy problem. With the technical advance and increasing demand for electricity, wind turbine has been developed from land to deep water with a larger capacity and structural scale. The length of wind turbine rotor blades is also enlarged for capturing more wind energy (see Fig.1). As the blade becoming longer, the flexibility of blade structure is also increased, and the blade deformation seems to be more complex.

In the process of operation, the blade is subjected to gravity, centrifugal force, and aerodynamic force. These forces cause the blade deformed at four different directions including longitudinal vibration (named axial extension), out of-plane bend (named flap), in-plane/edgewise bend (named lead/lag) and torsion [1]. The aeroelastic response of wind turbine blades is influenced by the structural coupling between bending and torsion of the blade. Bending–torsion coupling creates a feedback between the aerodynamic forces, which induce bending moments in the blade, and the blade torsion, which is directly related to the angle of attack and thus the aerodynamic forces [2]. Usually there are two kinds of models of blade to

study the aeroelastic problem. One of the models is to concentrate the elasticity of the blade to the root, and the whole blade is taken as a rigid body. It seems that the rigid blade is installed on a spring. Chopra and Dugundji [3] studied the nonlinear dynamic behavior and stability problem of the blade by the rigid body model considering the flap-motion, lead-lag motion and feathering motion. But the other parts of the wind turbine such as nacelle and tower were all neglected. Bir and Stol [4][5] examined the operating modes of a two-bladed teetered wind turbine which is modeled with seven degrees of freedom. The modal parameters were extracted by the Floquet approach. However, the rigid body model is only suitable for small wind turbine blades. As for large wind turbine blades, the airfoil of blade section and pre-twist angle vary greatly along the spanwise direction. The deformation of the blade is also increased. The modal shape, geometry, and airfoil distribution of the blade cannot be accurately described by the rigid body model. It is more reasonable to use the flexible body model to study the vibration of large wind turbine blades. Larsen et al[6] derived the non-linear partial differential equations of motion by considering the blade as a Bernoulli-Beam. Kallesøe [7] establish the nonlinear equations of bending and torsion motion of a rotor blade including the effects from gravity, pitch action and varying rotor speed. Li et al [1] put forward a mathematical model describing the nonlinear vibration of horizontal axis wind turbine blades, and the structural damping of the blade was considered.

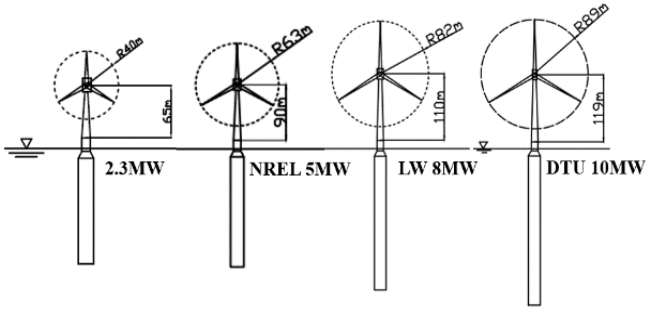

Figure1 Rotor radius of floating offshore wind turbine

Although a lot of research work has been done on the blade modeling of onshore wind turbines. There is little study about the offshore wind turbine blade modeling and the effect of platform motion on the blade deflection. In this paper, Hodges–Dowell's [8] partial differential equations of blade motion are extended by considering the whole wind turbine system including the platform motion, the nacelle yaw and the rotor rotation, except for the deflection of tower. The nonlinear equations of motion for the elastic bending and torsion of wind turbine blades is derived to study the natural properties. The natural frequencies and mode shapes of a rotating blade at different rotor speed are calculated. The analytical model proposed in this paper can provide a basis for the analysis of blade vibration and aeroelastic stability for floating offshore wind turbines in the future work.

COORDINATE SYSTEMS AND TRANSFORMATION

Several coordinate systems will be used to describe the configuration and motion of the wind turbine system (see Fig. 2). The orthogonal axes system X_0, Y_0, Z_0 and associated unit vectors $\vec{I}_0, \vec{J}_0, \vec{K}_0$ are fixed in the inertial frame. The origin of the system is point O_0. The orthogonal axes system X_1, Y_1, Z_1 is rigidly attached to the support platform which is used to define the translational (surge and heave) and rotational (pitch) motions of the platform. Its origin O_1 located at the mean sea level. The transformation matrix from $X_0Y_0Z_0$ to $X_1Y_1Z_1$ is given in the equation (1).

$$\begin{bmatrix} \mathbf{I_1} \\ \mathbf{J_1} \\ \mathbf{K_1} \end{bmatrix} = \begin{pmatrix} \cos\theta_{pitch} & 0 & -\sin\theta_{pitch} \\ 0 & 1 & 0 \\ \sin\theta_{pitch} & 0 & \cos\theta_{pitch} \end{pmatrix} \begin{bmatrix} \mathbf{I_0} \\ \mathbf{J_0} \\ \mathbf{K_0} \end{bmatrix} \tag{1}$$

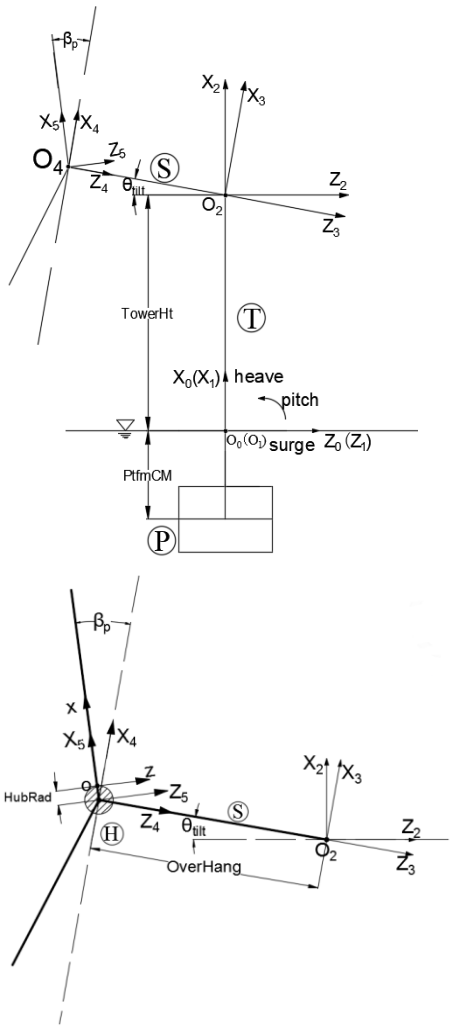

Figure 2 Description of the coordinate systems for FOWT

Transfer the coordinate system $X_1Y_1Z_1$ along with the X_1-axis. Then the orthogonal axes system X_2, Y_2, Z_2 is obtained

with origin O_2 at the tower top. The tower deflection can be expressed by X_2, Y_2, Z_2. However, the flexibility of tower is negligible here now, the coordinate system $X_1Y_1Z_1$ and $X_2Y_2Z_2$ are identical except for the position of the origin. The coordinate system $X_3Y_3Z_3$ is used to describe the motion of nacelle, which is first rotated about the X_2-axis with the angle θ_{yaw}. Hereafter system $X_3Y_3Z_3$ is rotated θ_{tilt} about the Y_3-axis, yielding a transformation matrix between coordinate system $X_2Y_2Z_2$ and $X_3Y_3Z_3$. The origin of the two systems are both point O_2. Three blade wind turbines usually don't have tilt motion. θ_{tilt} is the tilt angle of the rotor shaft from the nominally horizontal plane and it is constant.

$$\begin{bmatrix}\mathbf{I}_3\\ \mathbf{J}_3\\ \mathbf{K}_3\end{bmatrix}=\begin{pmatrix}\cos\theta_{\text{tilt}} & 0 & -\sin\theta_{\text{tilt}}\\ 0 & 1 & 0\\ \sin\theta_{\text{tilt}} & 0 & \cos\theta_{\text{tilt}}\end{pmatrix}\begin{pmatrix}1 & 0 & 0\\ 0 & \cos\theta_{\text{yaw}} & \sin\theta_{\text{yaw}}\\ 0 & -\sin\theta_{\text{yaw}} & \cos\theta_{\text{yaw}}\end{pmatrix}\begin{bmatrix}\mathbf{I}_2\\ \mathbf{J}_2\\ \mathbf{K}_2\end{bmatrix} \quad (2)$$

Since the shaft in this model is assumed to be stiff, the only transformation between system $X_3Y_3Z_3$ and system $X_4Y_4Z_4$ is a rotation about the Z_3 (or Z_4) -axis at constant angular velocity Ω. The transformation matrix of these two systems is showed in equation (3). The plane containing X_4 and Y_4 is called the reference plane, or plane of rotation. The origin O_4 of system $X_4Y_4Z_4$ is located at the intersection of the rotor axis and the plane of rotation (non-coned rotors) or the apex of the cone of rotation (coned rotors).

$$\begin{bmatrix}\mathbf{I}_4\\ \mathbf{J}_4\\ \mathbf{K}_4\end{bmatrix}=\begin{pmatrix}\cos\psi & \sin\psi & 0\\ -\sin\psi & \cos\psi & 0\\ 0 & 0 & 1\end{pmatrix}\begin{bmatrix}\mathbf{I}_3\\ \mathbf{J}_3\\ \mathbf{K}_3\end{bmatrix} \quad (3)$$

where the rotation angle $\psi=\int_0^t \Omega dt$ for t second.

The X_5-axis, which lies along the elastic axis of the undeformed beam, is inclined to the plane of rotation (and to the X_4 axis) at the pre-cone angle β_p (negative as shown in Fig. 2). So the relationship between the two systems $X_4Y_4Z_4$ and $X_5Y_5Z_5$ is:

$$\begin{bmatrix}\mathbf{I}_5\\ \mathbf{J}_5\\ \mathbf{K}_5\end{bmatrix}=\begin{pmatrix}\cos\beta_{\text{p}} & 0 & -\sin\beta_{\text{p}}\\ 0 & 1 & 0\\ \sin\beta_{\text{p}} & 0 & \cos\beta_{\text{p}}\end{pmatrix}\begin{bmatrix}\mathbf{I}_4\\ \mathbf{J}_4\\ \mathbf{K}_4\end{bmatrix} \quad (4)$$

Translating the $X_5Y_5Z_5$ system from the apex of the cone of rotation to the centroid of the blade root (point o), a new system *xyz* and the corresponding unit vectors $\vec{i}, \vec{j}, \vec{k}$ are established. The *xyz* system coincides with the $X_5Y_5Z_5$ system except for the location of origin. Here the radius of the rigid hub, HubRad, is considered.

The elastic deformation of a FOWT blade is shown in Figure 3. There are four components of deformation including axial extension, flap, lead/lag (in-plane/edgewise bending) and torsion. These deformations are described by the displacements of the elastic axis u, v, w, parallel to $\vec{i}, \vec{j}, \vec{k}$ respectively, and the torsion angle ϕ with respect to $\vec{i}'$ axis. A point on the elastic axis that is located at x, 0, 0 in the x, y, z coordinate system before deformation is located at x+u, v, w after deformation. The blade cross section is assumed to be symmetric with respect to the chord. Thus the center of mass, shear center and aerodynamic center of the blade section all locate on the chord line. The η and ζ axes shown in Figure 4 are the local coordinate system of the cross section. The origin of this system locates at the shear center. The η and ζ axes are inclined relative to the y and z axes at a twist angle θ ($\theta=\theta_0+\theta_t$, θ_0 is the setting angle and θ_t is the pre-twist angle). The angle of twist of the cross-section changes from θ about the x axis to $\theta+\phi$ about the x' axis.

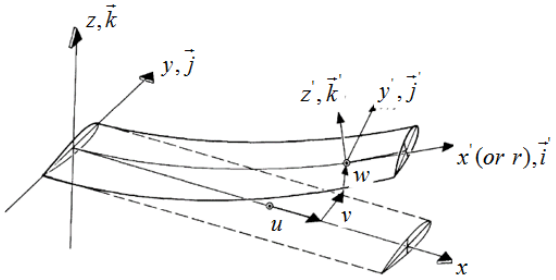

Figure 3 Elastic deformation of the blade[8]

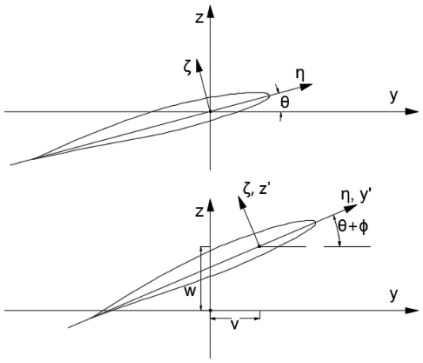

Figure 4 Cross-section coordinates before and after deformation

The complicated transformation from coordinate xyz undeformed system to $x'y'z'$ deformed system is given by Ref 8.

$$\begin{bmatrix}\mathbf{i}'\\ \mathbf{j}'\\ \mathbf{k}'\end{bmatrix}=\begin{pmatrix}1-\frac{1}{2}v'^2-\frac{1}{2}w'^2 & v' & w'\\ -[v'\cos(\theta+\phi)+w'\sin(\theta+\phi)] & \cos(\theta+\phi+v'w')(1-\frac{v'^2}{2}) & \sin(\theta+\phi)(1-\frac{w'^2}{2})\\ v'\sin(\theta+\phi)-w'\cos(\theta+\phi) & -\sin(\theta+\phi+v'w')(1-\frac{v'^2}{2}) & \cos(\theta+\phi)(1-\frac{w'^2}{2})\end{pmatrix}\begin{bmatrix}\mathbf{i}\\ \mathbf{j}\\ \mathbf{k}\end{bmatrix} \quad (5)$$

where $v'=\dfrac{\partial v}{\partial x}$ and $w'=\dfrac{\partial w}{\partial x}$.

DERIVATION OF GOVERNING EQUATIONS

The equations of motion for a FOWT blade rotating at constant speed are obtained from Hamilton's principle. The rotor blade can be regard as a long, slender, homogeneous, isotropic beam. The external forces acting on the beam are characterized by a set of generalized distributed loads.

The expression of generalized Hamilton principle is:

$$\int_{t1}^{t2}[\delta(U-T)-\delta W]dt=0 \quad (6)$$

where U is the strain energy, T is the kinetic energy, and δW is the virtual work of the external forces. Suitable expressions for δU , δV , and δW are now determined and then combined to give the desired equations.

Strain energy contributions

The blade is regard as a long slender beam. According to Ref. 8, the nonlinear strain–displacement relation of the normal strain ε_{xx} as well as the shear strain component $\varepsilon_{x\eta}$ and $\varepsilon_{x\zeta}$ are obtained as:

$$\begin{cases}\varepsilon_{xx}=u'+\dfrac{v'^2}{2}+\dfrac{w'^2}{2}+(\eta^2+\zeta^2)(\theta'\phi'+\dfrac{\phi'^2}{2})\\ \qquad -v''[\eta\cos(\theta+\phi)-\zeta\sin(\theta+\phi)]\\ \qquad -w''[\eta\sin(\theta+\phi)+\zeta\cos(\theta+\phi)]\\ \varepsilon_{x\eta}=-\zeta\phi'\\ \varepsilon_{x\zeta}=\eta\phi'\end{cases} \quad (7)$$

The variation of the strain energy U is:

$$\delta U=\int_0^R\iint_A(E\varepsilon_{xx}\delta\varepsilon_{xx}+G\varepsilon_{x\eta}\delta\varepsilon_{x\eta}+G\varepsilon_{x\zeta}\delta\varepsilon_{x\zeta})d\eta d\zeta\ dx \quad (8)$$

where E is the Young's modulus of elasticity, G is the shear modulus.

Kinetic energy contributions

The derivation of kinetic energy of a blade is something different from the previous work. Because the effect of platform motion (surge, heave, pitch) for FOWT is considered in this part.

Kinematics

The whole analytical system consists of six rigid body (earth, support platform, tower, nacelle, shaft and hub) and three flexible blades. The hub is rigidly connected with the shaft. Thus they can be regard as one rigid body. Applying the addition theorem for angular velocities [9] yields the following form of the angular velocity of hub in the inertial frame

$${}^{\mathrm{E}}\omega^{\mathrm{H}}={}^{\mathrm{E}}\omega^{\mathrm{P}}+{}^{\mathrm{P}}\omega^{\mathrm{T}}+{}^{\mathrm{T}}\omega^{\mathrm{N}}+{}^{\mathrm{N}}\omega^{\mathrm{H}} \quad (9)$$

where ${}^{\mathrm{E}}\omega^{\mathrm{P}}$ is the angular velocity of the platform in the inertial frame. Because the tower is rigidly attached with platform and the flexibility of tower is also ignored. The angular velocity of tower top relative to the platform equals zero. In other words, ${}^{\mathrm{P}}\omega^{\mathrm{T}}=0$. The angular velocity of the nacelle relative to the tower-top base plate, ${}^{\mathrm{T}}\omega^{\mathrm{N}}$, has a component associated with the rate of yaw. ${}^{\mathrm{N}}\omega^{H}$ is the angular velocity of the shaft (or hub) to nacelle which is related to the time derivative of the azimuth angle. The previous four terms can be combined to give the following form of the angular velocity of the hub in the inertial reference frame:

$${}^{\mathrm{E}}\omega^{\mathrm{H}}=\dot{\theta}_{\mathrm{pitch}}\,\mathbf{J_0}+\dot{\theta}_{\mathrm{yaw}}\,\mathbf{I_2}+\Omega\mathbf{K_4} \quad (10)$$

To simply the analysis, ${}^{\mathrm{E}}\omega^{\mathrm{H}}$ can be written as the following form:

$${}^{\mathrm{E}}\omega^{\mathrm{H}}=[A_1\quad A_2\quad A_3]\begin{bmatrix}\mathbf{i}\\ \mathbf{j}\\ \mathbf{k}\end{bmatrix} \quad (11)$$

The explicit expression of A_1, A_2 and A_3 can be obtained by substituting equations (1) ~ (4) into equation (10).

The velocity of the platform (Point O_1) in the inertial frame is:

$${}^{\mathrm{E}}v^{O_1}=\dot{X}_{heave}\,\mathbf{I_0}+\dot{Z}_{surge}\,\mathbf{K_0} \quad (12)$$

where $\dot{X}_{heave}$ and $\dot{Z}_{surge}$ represent the velocity of platform heave and surge respectively.

The velocity of the tower top (point O_2) in the inertial frame is:

$$\begin{aligned}{}^{E}v^{O_2}&={}^{E}v^{O_1}+{}^{E}\omega^{T}\times\mathbf{r}^{\mathbf{O_1O_2}}\\ &={}^{E}v^{O_1}+({}^{E}\omega^{P}+{}^{P}\omega^{T})\times\mathbf{r}^{\mathbf{O_1O_2}}\end{aligned} \quad (13)$$

where the position victor $\mathbf{r}^{\mathbf{O_1O_2}}=TowerHt\ \mathbf{I_1}$. $TowerHt$ is the distance from mean sea level to the top of the tower.

The velocity of the apex of the cone of rotation (point O_4) in the inertial frame is:

$${}^{E}v^{O_4}={}^{E}v^{O_2}+{}^{E}\omega^{H}\times\mathbf{r}^{\mathbf{O_2O_4}} \quad (14)$$

where the position victor $\mathbf{r}^{\mathbf{O_2O_4}}=OverHang\mathbf{K_3}$. $OverHang$ is the distance along the rotor shaft from the X_3Y_3 plane to the rotor apex.

The velocity of the centroid of the blade root (point o) in the inertial frame is:

$${}^{E}v^{o}={}^{E}v^{O_4}+{}^{E}\omega^{H}\times\mathbf{r}^{\mathbf{O_4o}} \quad (15)$$

where the position victor $\mathbf{r}^{O_4 o} = HubRad\ \mathbf{i}$. *HubRad* is the distance from the apex of the cone of rotation to the centroid of blade root along the pitch axis. To make it easier to understand, the expression of some parameters here is the same as that in *FAST Code*.

Like the angular velocity, the term ${}^{E}v^{O}$ can be simplified as:

$$ {}^{E}v^{O} = [B_1 \quad B_2 \quad B_3] \begin{bmatrix} \mathbf{i} \\ \mathbf{j} \\ \mathbf{k} \end{bmatrix} \tag{16} $$

The explicit expression of B_1 , B_2 and B_3 can also be obtained by substituting equations (1) ~ (4) and (10) into equation (16). Here the effect of platform motion and other parts of the wind turbine system on blade dynamic response are all considered.

Kinetic energy

The vector position of a generic point S on the undeformed beam is given by (x, y, z) with respect to the unit vectors $\vec{i}, \vec{j}, \vec{k}$ where (x, 0, 0) is the elastic axis. After the blade deformed, the position of point S can be given by (x_1 , y_1 , z_1). The high order terms have been ignored. Only the first and second order terms are retained.

$$ \begin{cases} x_1 = x + u - v'[\eta\cos(\theta+\phi) - \zeta\sin(\theta+\phi)] \\ \qquad - w'[\eta\sin(\theta+\phi) + \zeta\cos(\theta+\phi)] \\ y_1 = v + \eta\cos(\theta+\phi) - \zeta\sin(\theta+\phi) \\ z_1 = w + \eta\sin(\theta+\phi) + \zeta\cos(\theta+\phi) \end{cases} \tag{17} $$

The velocity of point S in the inertial frame is:

$$ {}^{E}v^{S} = {}^{H}v^{S} + {}^{E}v^{o} + {}^{E}\omega^{H} \times \mathbf{r}^{oS} \tag{18} $$

where ${}^{H}v^{S}$ is the velocity of the point S relative to the reference frame xyz, which can be written as:

$$ {}^{H}v^{S} = \dot{x}_1\mathbf{i} + \dot{y}_1\mathbf{j} + \dot{z}_1\mathbf{k} \tag{19} $$

By substituting equations (11), (16) and (19) into equation (18), one can obtain the expression of ${}^{E}v^{S}$:

$$ \begin{aligned} {}^{E}v^{S} = {} & (\dot{x}_1 + B_1 + A_2 z_1 - A_3 y_1)\mathbf{i} + (\dot{y}_1 + B_2 + A_3 x_1 - A_1 z_1)\mathbf{j} \\ & + (\dot{z}_1 + B_3 + A_1 y_1 - A_2 x_1)\mathbf{k} \end{aligned} \tag{20} $$

The variation of the kinetic energy T of the rotating blade is:

$$ \delta T = \int_0^L \iint_A \rho\ {}^{E}v^{S}\ \delta\,{}^{E}v^{S}\ d\eta d\zeta\ dx \tag{21} $$

where L is the length of flexible blade, measured from the centroid of blade root to blade tip. The variation of the velocity of point S is:

$$ \begin{aligned} \delta\,{}^{E}v^{S} = {} & (\delta\dot{x}_1 + A_2\delta z_1 - A_3\delta y_1)\mathbf{i} + (\delta\dot{y}_1 + A_3\delta x_1 - A_1\delta z_1)\mathbf{j} \\ & + (\delta\dot{z}_1 + A_1\delta y_1 - A_2\delta x_1)\mathbf{k} \end{aligned} \tag{22} $$

It is assumed that $\delta\,{}^{E}v^{o}$ and $\delta\,{}^{E}\omega^{H}$ are both zero for a qusi-static method.

Nonlinear equations of motion

The virtual work δW of the nonconservative forces can be expressed as:

$$ \delta W = \int_0^L (F_x\delta u + F_y\delta v + F_z\delta w + M_\phi\delta\phi + M_y\delta w' + M_z\delta v')dx \tag{23} $$

where F_x , F_y , F_z and M_x , M_y , M_z represent the resultant distributed forces and moments (including gravitational, aerodynamic and other external loading) in x-, y- and z-directions respectively.

By substituting equations (8), (21) and (23) into equation (6), the total variational equation in terms of u, v, w, and ϕ can be obtained. For arbitrary, admissible variations δu , δv , δw and $\delta\phi$, the coefficients of the variations must vanish in the integrand for all x from 0 to L. This condition will yield four nonlinear partial differential equations. After linearization, the four governing equations of the axial motion, flap, lead/lag and torsion are as follows:

The axial motion:

$$ -\mathrm{T}' - C^{(u)}(\dot{\kappa}, \ddot{\kappa}, \dot{\kappa}', \ddot{\kappa}') - D^{(u)}(\kappa, \kappa') = F_x \tag{24} $$

The flap motion:

$$ \begin{aligned} & \{(EI_z\sin^2\theta + EI_y\cos^2\theta)w'' + (EI_z - EI_y)(v''\sin\theta\cos\theta + v''\phi\cos 2\theta + w''\phi\sin 2\theta) - Te_A(\sin\theta + \phi\cos\theta) \\ & + EAe_A k_A^2\theta'\phi'\sin\theta - EAe_A^2(v''\sin\theta\cos\theta + w''\sin^2\theta + v''\phi\cos 2\theta + w''\phi\sin 2\theta) - EB_2^*\theta'\phi'\sin\theta\}'' - (Tw')' \\ & + C^{(w)}(\dot{\kappa}, \ddot{\kappa}, \dot{\kappa}', \ddot{\kappa}') + D^{(w)}(\kappa, \kappa') = F_z - M_y' \end{aligned} \tag{25} $$

The lead/lag motion:

$$ \begin{aligned} & \{(EI_z\cos^2\theta + EI_y\sin^2\theta)v'' + (EI_z - EI_y)[\sin\theta\cos\theta w'' - 2\phi v''\sin\theta\cos\theta + (\cos^2\theta - \sin^2\theta)\phi w'']] \\ & - EB_2^*\theta'\phi'\cos\theta - [Te_A(\cos\theta - \phi\sin\theta) - EAk_A^2e_A\theta'\phi'\cos\theta + EAe_A^2(v''\cos^2\theta - v''\phi\sin 2\theta \\ & + w''\sin\theta\cos\theta + w''\phi\cos 2\theta]\}'' - (Tv')' + C^{(v)}(\dot{\kappa}, \ddot{\kappa}, \dot{\kappa}', \ddot{\kappa}') + D^{(v)}(\kappa, \kappa') = F_y - M_z' \end{aligned} \tag{26} $$

The torsion motion:

$$\begin{aligned}&-\{k_A^2(\theta+\phi)'[T-EAk_A^2\theta'\phi'+EAe_A(v''\cos\theta+w''\sin\theta)]+EB_1^{*}\theta'^2\phi'-EB_2^{*}\theta'(v''\cos\theta+w''\sin\theta)\}'-(GJ\phi')'\\&-e_A(w''\cos\theta-v''\sin\theta)[T-EAk_A^2\theta'\phi'+EAe_A(v''\cos\theta+w''\sin\theta)]+(EI_z-EI_y)[(w''^2-v''^2)\cos\theta\sin\theta+v''w''\cos 2\theta]\\&+C^{(\phi)}(\ddot{\kappa},\ddot{\kappa},\dot{\kappa}',\ddot{\kappa}')+C^{(\phi)}(\kappa,\kappa')=M_\phi\end{aligned} \tag{27}$$

where

$$T=EA\left\{u'+\frac{v'^2}{2}+\frac{w'^2}{2}+k_A{}^2\theta'\phi'-e_A[v''\cos(\theta+\phi)+w''\sin(\theta+\phi)]\right\} \tag{28}$$

The associated boundary conditions are:

$$u\big|_{x=0}=v\big|_{x=0}=w\big|_{x=0}=\phi\big|_{x=0}=0,\quad u'\big|_{x=0}=v'\big|_{x=0}=w'\big|_{x=0}=\phi'\big|_{x=L}=0,\quad v''\big|_{x=L}=w''\big|_{x=L}=0,\ T\big|_{x=L}=0,\ T\big|_{x=0}=T_{\max}.$$

In equations (24) ~ (27), the symbol κ represents taking all four variables u, w, v and ϕ. The expression of $C^{(\kappa)}$ and $D^{(\kappa)}$ are presented in the Appendix A.

Before solving for the motion equations, it is more convenient to eliminate u from the equation (24) ~ (27). According to equations (24) and (28), u can be expressed by terms T, v, w, and ϕ. The expression of T can be written as:

$$\mathrm{T}=\int_x^R (F_x+C^{(u)}(\ddot{\kappa},\ddot{\kappa},\dot{\kappa}',\ddot{\kappa}')+D^{(u)}(\kappa,\kappa'))dx \tag{29}$$

Thus u' can be solved. The expression of $\dot{u}$ can be obtained by integrating u' over x and then differentiating with respect to t.

VERIFICATION OF THE ANALYTICAL MODEL

Method of solution

Based on the normal mode summation method, the blade deformation can be expressed as a linear sum of known shapes of the dominant normal vibration modes [9].

$$\begin{cases}v=\sum_{k=1}^{Nv}\gamma_{vk}(x)q_{vk}(t)\\ w=\sum_{k=1}^{Nw}\gamma_{wk}(x)q_{wk}(t)\\ \phi=\sum_{k=1}^{N_\phi}\gamma_{\phi k}(x)q_{\phi k}(t)\end{cases} \tag{30}$$

where $q_{vk}(t)$, $q_{wk}(t)$ and $q_{\phi k}(t)$ are the generalized coordinates associated with the modal function $\gamma_{vk}(x)$, $\gamma_{wk}(x)$ and $\gamma_{\phi k}(x)$ respectively. N_v, N_w and N_ϕ are the number of modal functions used to describe edgewise, flapwise and torsion motion respectively.

Alternatively, the deflection of the blade can also be expressed using N other functions $\bar{\gamma}(x)$, which satisfy the boundary conditions and not unique to each normal mode, according to the *assumed-modes method*. The modal function can be written as linear combination of the shape function：

$$\gamma_{vk}=\sum_{j=1}^{N_v}a_j\bar{\gamma}_{vj},\ \gamma_{wk}=\sum_{j=1}^{N_w}b_j\bar{\gamma}_{wj},\ \gamma_{\phi k}=\sum_{j=1}^{N_\phi}c_j\bar{\gamma}_{\phi j} \tag{31}$$

The shape functions of different motion are:

$$\begin{cases}\bar{\gamma}_{vj}(x)=(x/L)\wedge(j+NP\text{-}1)\\ \bar{\gamma}_{wj}(x)=(x/L)\wedge(j+NP\text{-}1)\\ \bar{\gamma}_{\phi j}(x)=\sin\dfrac{(2j\text{-}1)\pi}{2L}x\end{cases} \tag{32}$$

where the lateral deflection (edgewise and flapwise) of blade is assumed to be expressible as a polynomial and NP is the order of the first coefficient. To satisfy the geometric boundary conditions, NP must be no smaller than two.

Substitute equations (30) (31) and (32) into equations (25) ~ (27). Based on Galerkin's method, the modal motion equations can be obtained through weighted integral by the shape function with respect to x.

$$\begin{cases}\int_0^L E_1(v,w,\phi)\gamma_{vi}(x)dx=0\\ \int_0^L E_2(v,w,\phi)\gamma_{wi}(x)dx=0\\ \int_0^L E_3(v,w,\phi)\gamma_{\phi i}(x)dx=0\end{cases} \tag{33}$$

where $E_1(v,w,\phi)$, $E_2(v,w,\phi)$ and $E_3(v,w,\phi)$ are the expression of equations (25), (26) and (27) after moving the right side terms to the left. The velocity terms and static deformation is neglected to analysis the natural properties of the blade. The modal motion equations can be written as:

$$\left[-\omega^2\mathbf{M}+\mathbf{K}\right]\cdot\left[a_1,...,a_{N_v},b_1,...b_{N_w},c_1,...c_{N_\phi}\right]^T=0_{(N_v+N_w+N_\phi)\times 1} \tag{34}$$

The coefficients $a_1,...,a_{N_v},b_1,...b_{N_w},c_1,...c_{N_\phi}$ cannot equal to zero at the same time, thus $\left|-\omega^2\mathbf{M}+\mathbf{K}\right|=\mathbf{0}$ .The natural frequencies and the associated undamped modal function can be obtained by solving the equation.

Verification of the model

The NREL 5MW wind turbine blade was chosen as an example to validate the analytical model in this paper. The geometric and material properties of the blade can be found in

Ref. [10]. FAST uses a program called Modes to generate mode shapes of blades. Here the program Modes was also used to validate the model. The number of modal functions in Modes and current model are set the same, which is $N_v = N_w = 5, N_\phi = 3$.

Reference [11] did an eigen analysis by ADAMS, based on a multi-body model. The comparison of the results for a static blade are shown in table1. And the comparison of mode shapes can be found in Figure 5.

The results in table1 showed that the flapwise and edgewise frequencies calculated by the current model are in good agreement with the associated results of Modes and Ref. [11]. The mode shapes also agree well. The natural frequency and mode shape of torsion motion was also calculated which is not included in Modes. Usually the torsional mode does not occur alone. It is coupled with other modes. The coupling of all kinds of deformation has an important influence on the aerodynamic stability of the blade.

Table 1 Comparison of the natural properties for a static blade

Natural Frequency(Hz)	Modes(FAST)	ADAMS [11]	Current model
First flapwise	0.6830	0.6745	0.6824
Firsr edgewise	1.0968	1.1033	1.0925
Second flapwise	1.9909	1.8394	1.9921
Second edgewise	4.0714	3.8997	4.0464
First torsion	-	-	5.7446

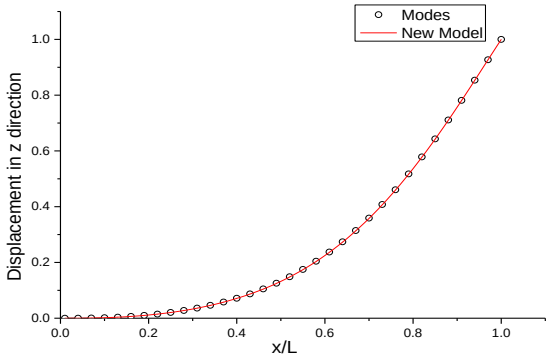

(a) First flapwise mode shape

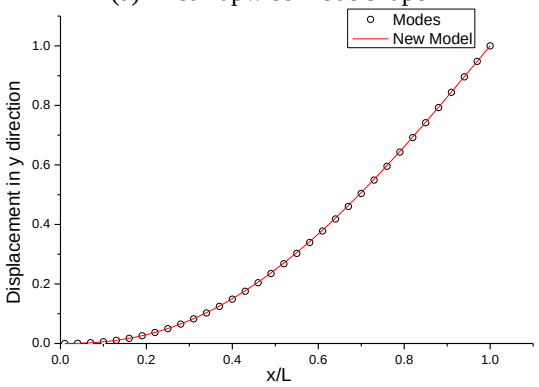

(b) First edgewise mode shape

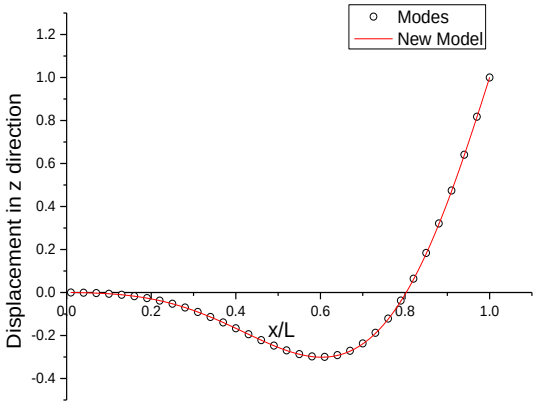

(c) Second flapwise mode shape

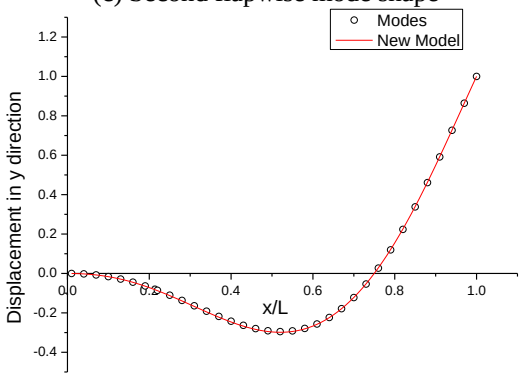

(d) Second edgewise mode shape

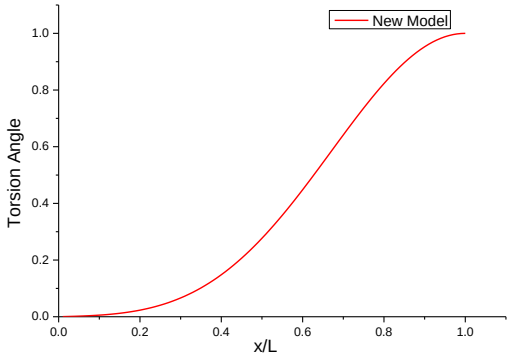

(e) First torsion mode shape

Figure 5 Comparison of mode shapes with FAST-Modes

Eigen analysis of the blade at different rotational speed

The rotating blade is deformed by the effect of the centrifugal force. Because of the coupling between rigid motion and elastic deflection, the stiffness of the blades is increased. This phenomenon is called dynamic stiffening. The natural frequency of a rotating blade at different rotational speed was calculated. The geometric and material properties of the blade have been given previously. For different rotational speed, the value of coefficient A_i and B_i (i=1,2,3) will be changed. The natural frequencies can be obtained by solving equation (34). The results are shown in Table2 and the natural mode shapes can be found in Figure 6.

Table 2 Natural frequency of rotated blade(Hz)

Rotor Speed	Mode Shape			
	First Flapwise	Second Flapwise	First Edgewise	Second Edgewise
0	0.6824	1.9921	1.0925	4.0464
3r/min	0.7005	2.0304	1.0967	4.0584
6r/min	0.7442	2.1328	1.1088	4.0933
9r/min	0.7965	2.2732	1.1273	4.1484
12r/min	0.8486	2.4300	1.1504	4.2207
15r/min	0.8983	2.5923	1.1763	4.3072

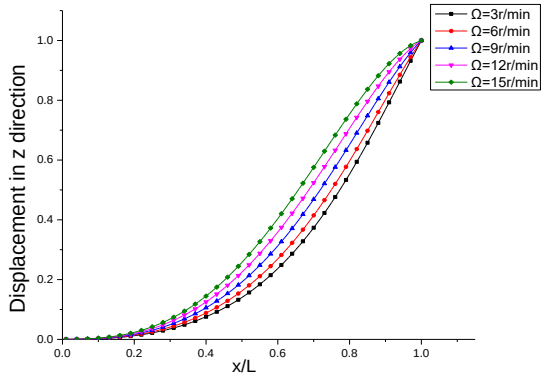

(a) First flapwise mode shape

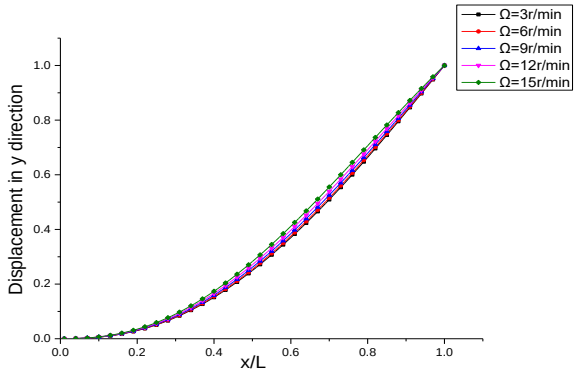

(b) First edgewise mode shape

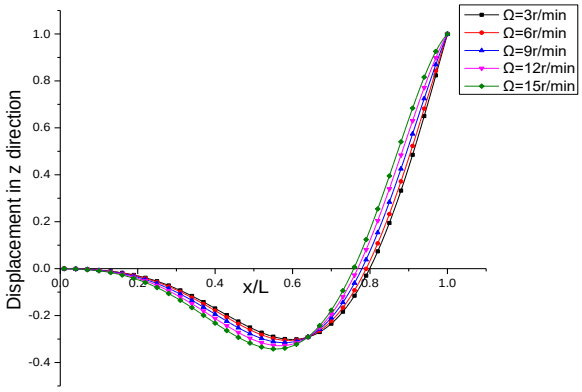

(c) Second flapwise mode shape

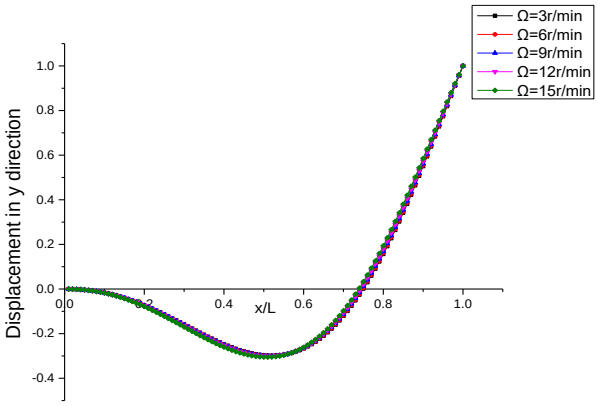

(d) Second edgewise mode shape

Figure 6 Mode shapes at different rotational speed

It can be found that as the rotational speed increased, the natural frequency significantly changed. When the rotor speed increased from 0 to 15 r/min, the frequency of fist flapwise and second flapwise mode increased by 0.2159Hz,31.6% and 0.6002Hz,30.1%, respectively. For the edgewise mode, as the rotor speed changed, the first edgewise frequency increased 0.0838Hz, 7.7% and the second edgewise frequency increased 0.2608Hz, 6.4%. The phenomenon is in accordance with the Ref. 12. It also can be seen that the change of rotor speed has a greater effect on the flapwise motion than edgewise. Meanwhile the frequency of low-order mode is easier to be changed as the rotor speed increased. In Fig.6, the flapwise mode shapes change more obviously than the edgewise. Basically, all the mode shapes don't change a lot at different rotor speed.

CONCLUSION AND FUTURE WORK

In this paper, an analytical model for floating offshore wind turbine blades is put forward based on Hamilton's principle. The bending-torsion coupling effect is considered to derive the nonlinear motion equations. The governing equations of flapwise and edgewise deformation, the torsion as well as axial extension of the blades are obtained. NREL 5MW wind turbine blade is taken as an example to validate the analytical model. The frequencies and shapes of the natural modes of blade vibration are compared to results from FAST-Modes and ADAMS (the multi-body model), showing good agreement. The accuracy of the analytical model in this paper is validated. The natural frequencies of both the flapwise and edgewise vibration is getting lager as the rotor speed increased because of the effect of dynamic stiffening. However, the change of mode shapes is not so obviously as that of frequency. Usually, the rotor speed has little effect on the mode shapes, but it will have a significant effect on the frequency of vibration.

Based on the analytical model proposed in this paper, we can do more research work in the next step. We plan to combine the structural model in this paper with the aerodynamic model to study the aeroelastic properties of the blade and analyze the effect of different structural parameters

on blade dynamic response. At present, the wind turbine is fixed to study the natural properties of the blades. While, in the next step, the hydrodynamic load will be included to calculate the platform motion which can be regard as an input of the structural model. And then we can further explore the influence of platform motion on blade nonlinear dynamic response. The flexibility of tower can also be considered at that time. According to these research work, the instability mechanisms of wind turbine blades vibration can be revealed. And some suggestions about designs and control strategy to avoid instabilities can also be provided.

ACKNOWLEDGMENTS

The research described in this paper was financially supported by Nation Natural Science Foundation of China (Project No. 51479134), and Natural Science Foundation of Tianjin (No.16JCYBJC21200). These sources of support are gratefully acknowledged. The support provided by China Scholarship Council (CSC) during a visit of Xiaoqi QU to NTNU is highly acknowledged.

REFERENCES

[1] Li L, Li Y H, Liu Q K, et al. A mathematical model for horizontal axis wind turbine blades [J]. Applied Mathematical Modelling, 2014, 38(11): 2695-2715.

[2] Stäblein A R, Hansen M H, Pirrung G. Fundamental aeroelastic properties of a bend–twist coupled blade section[J]. Journal of Fluids and Structures, 2017, 68: 72-89.

[3] Chopra I, Dugundji J. Non-linear dynamic response of a wind turbine blade[J]. Journal of sound and vibration, 1979, 63(2): 265-286.

[4] Bir G, Stol K. 'Modal Analysis of a Teetered-Rotor Wind Turbine using the Floquet Approach[C]//Proc. of 19th ASME Wind Energy Symp. 2000: 23-33.

[5] Stol K, Balas M, Bir G. Floquet modal analysis of a teetered-rotor wind turbine[J]. Transactions-American Society of Mechanical Engineering Journal of Solar Energy Engineering, 2002, 124(4): 364-371.

[6] Larsen J W, Nielsen S R K. Non-linear dynamics of wind turbine wings[J]. International Journal of Non-Linear Mechanics, 2006, 41(5): 629-643.

[7] Kallesøe B S. Equations of motion for a rotor blade, including gravity, pitch action and rotor speed variations[J]. Wind Energy, 2007, 10(3): 209-230.

[8] D.H. Hodges, E.H. Dowell, Nonlinear equations of motion for the elastic bending and torsion of twisted nonuniform rotor blades, Technical Note D-7818, NASA, 1974.

[9] Jonkman J M. Modeling of the UAE wind turbine for refinement of FAST _ AD[R]. National Renewable Energy Lab., Golden, CO (US), 2003.

[10] Jonkman J, Butterfield S, Musial W, et al. Definition of a 5-MW reference wind turbine for offshore system development[R]. National Renewable Energy Laboratory (NREL), Golden, CO., 2009.

[11] Cantang Zhong. Analyse the modal dynamics of horizontal axis wind by multi-body model [D]. Guangdong University of Technology, 2015.

[12] Lee S Y, Lin S M, Wu C T. Free vibration of a rotating non-uniform beam with arbitrary pretwist, an elastically restrained root and a tip mass[J]. Journal of Sound and Vibration, 2004, 273(3): 477-492.

ANNEX A

EXPRESSION OF THE COEFFICIENT TERMS IN MOTION EQUATIONS

$$C^{(u)}(\dot{\kappa},\ddot{\kappa},\dot{\kappa}',\ddot{\kappa}') = 2A_3 m\dot{v} - 2A_2 m\dot{w} \tag{A.1}$$

$$D^{(u)}(\kappa,\kappa') = (A_2^2 + A_3^2)mx - A_1A_2mv - A_1A_3mw - A_1A_2me\cos(\theta+\phi) - A_1A_3me\sin(\theta+\phi) + (A_3B_2 - A_2B_3)m \tag{A.2}$$

$$\begin{aligned} C^{(w)}(\dot{\kappa},\ddot{\kappa},\dot{\kappa}',\ddot{\kappa}') = {} & m\ddot{w} + \ddot{\phi}me\cos\theta - 2A_2m\dot{u} + 2A_1m\dot{v} - 2A_1\dot{\phi}me\sin\theta + 2A_2\dot{v}'me\cos\theta + 2A_2\dot{w}me\sin\theta \\ & -[(2A_3\dot{v} - 2A_2\dot{w})me\sin\theta]' \end{aligned} \tag{A.3}$$

$$\begin{aligned} D^{(w)}(\kappa,\kappa') = {} & -(A_1^{\,2} + A_2^{\,2})mw - (A_1^{\,2} + A_2^{\,2})me(\sin\theta + \phi\cos\theta) + A_1A_3xm - A_1A_3v'me\cos\theta - A_1A_3w'me\sin\theta \\ & + A_2A_3mv + A_2A_3me(\cos\theta - \phi\sin\theta) - (A_2B_1 - A_1B_2)m + \{-[(A_2^2 + A_3^2)x + A_3B_2 - A_2B_3]me(\sin\theta + \phi\cos\theta) \\ & + A_1A_2vme\sin\theta + A_1A_2m(k_{m2}^2 - k_{m1}^2)(\cos\theta\sin\theta + \phi\cos 2\theta) + A_1A_3wme\sin\theta \\ & + A_1A_3m[k_{m2}^2\sin^2\theta + k_{m1}^2\cos^2\theta + (k_{m2}^2 - k_{m1}^2)\phi\sin 2\theta]\}' \end{aligned} \tag{A.4}$$

$$\begin{aligned} C^{(v)}(\dot{\kappa},\ddot{\kappa},\dot{\kappa}',\ddot{\kappa}') = {} & m\ddot{v} - \ddot{\phi}me\sin\theta + 2A_3m\dot{u} - 2A_1m\dot{w} - 2A_1\dot{\phi}me\cos\theta - 2A_3\dot{v}'me\cos\theta - 2A_3\dot{w}'me\sin\theta \\ & -[(2A_3\dot{v} - 2A_2\dot{w})me\cos\theta]' \end{aligned} \tag{A.5}$$

$$\begin{aligned} D^{(v)}(\kappa,\kappa') = {} & -(A_1^{\,2} + A_3^{\,2})mv - (A_1^{\,2} + A_3^{\,2})me\cos\theta + (A_1^{\,2} + A_3^{\,2})me\phi\sin\theta + A_1A_2mx - A_1A_2v'me\cos\theta - A_1A_2w'me\sin\theta \\ & + A_2A_3mw + A_2A_3me\sin\theta + A_2A_3me\phi\cos\theta - (A_1B_3 - A_3B_1))m + \{-(A_2^2 + A_3^2)mex(\cos\theta - \phi\sin\theta) \\ & + (A_2B_3 - A_3B_2)me(\cos\theta - \phi\sin\theta) + A_1A_2vme\cos\theta + A_1A_3m(k_{m2}^2 - k_{m1}^2)(\sin\theta\cos\theta + \phi\cos 2\theta) \\ & + A_1A_3wme\cos\theta + A_1A_2m[k_{m1}^2\sin^2\theta + k_{m2}^2\cos^2\theta + (k_{m1}^2 - k_{m2}^2)\phi\sin 2\theta]\}' \end{aligned} \tag{A.6}$$

$$\begin{aligned} C^{(\phi)}(\dot{\kappa},\ddot{\kappa},\dot{\kappa}',\ddot{\kappa}') = {} & -\dot{v}me\sin\theta + \ddot{\phi}mk_m^2 + 2A_1\dot{w}me\sin\theta + 2A_1\dot{v}me\cos\theta + \ddot{w}me\cos\theta + 2A_2\dot{v}'m(k_{m2}^2\cos^2\theta + k_{m1}^2\sin^2\theta) \\ & + 2A_3\dot{w}'m(k_{m2}^2\sin^2\theta + k_{m1}^2\cos^2\theta) + 2(A_3\dot{v}' + A_2\dot{w}')m(k_{m2}^2 - k_{m1}^2)\cos\theta\sin\theta \end{aligned} \tag{A.7}$$

$$\begin{aligned} D^{(\phi)}(\kappa,\kappa') = {} & A_1A_3xme(\cos\theta - \phi\sin\theta) - A_1A_2xme(\sin\theta + \phi\cos\theta) - (A_2^2 + A_3^2)xv'me\sin\theta + (A_2^2 + A_3^2)xw'me\cos\theta \\ & + (A_1^2 + A_3^2)vme\sin\theta - (A_1^2 + A_2^2)wme\cos\theta - A_2A_3wme\sin\theta + A_2A_3vme\cos\theta + (A_3B_2 - A_2B_3)w'me\cos\theta \\ & - (A_3B_2 - A_2B_3)v'me\sin\theta + (A_1A_3v' + A_1A_2w')m(k_{m1}^2 - k_{m2}^2)\cos 2\theta - (A_2B_1 - A_1B_2)me(\cos\theta - \phi\sin\theta) \\ & - (A_2^2 + A_3^2)m(k_{m2}^2 - k_{m1}^2)(\cos\theta\sin\theta + \phi\cos 2\theta) + 2(A_1A_2v' - A_1A_3w')m(k_{m2}^2 - k_{m1}^2)\cos\theta\sin\theta \\ & - (A_3B_1 - A_1B_3)me(\sin\theta + \phi\cos\theta) + A_2A_3m(k_{m2}^2 - k_{m1}^2)(\cos 2\theta - 2\phi\sin 2\theta) \end{aligned} \tag{A.8}$$